Electronic Supplementary Information

Three-Dimensional Multilayer Graphene Web for Polymer Nanocomposites with Exceptional Transport Properties and Fracture Resistance

*[1]Xi Shen, [1]Zhenyu Wang, [1]Ying Wu, [1]Xu Liu, [2]Yan-Bing He, [1]Qingbin Zheng, [2]Quan-Hong Yang, [2]Feiyu Kang, [1]Jang-Kyo Kim**

[1]Department of Mechanical and Aerospace Engineering, The Hong Kong University of Science and Technology, Clear Water Bay, Kowloon, Hong Kong

[2]Engineering Laboratory for Functionalized Carbon Materials, Graduate School at Shenzhen, Tsinghua University, Shenzhen 518055, China

*To whom the correspondence should be addressed: mejkkim@ust.hk

S1. Experimental methods

Fabrication of MGW/epoxy composites. The MGWs were grown on compressed Ni foams using the CVD method. Several layers of 1.6-mm-thick Ni foams (Heze Tianyu Technology Development Co. with a mesh density of 320 g/m^2) were stacked and compressed uniaxially into a 1.6 mm thick sheet using a hydraulic press. The compressed Ni foams were cut into rectangles of 60 mm x 90 mm, and sonicated in acetone for 3 h to remove any impurities. The cleaned Ni templates were rinsed using DI water and dried in an oven at 60 °C overnight. The CVD was carried out in a tube furnace (MTI dual zone sliding tube furnace, EQCCA1110-220). The compressed Ni foams were placed in a quartz tube,

which was then evacuated using a vacuum pump. The mixed gas flow of Ar (500 ml min^{-1}) and H_2 (200 ml min^{-1}) was introduced into the tube. The temperature of tube was increased to 1000 °C at a rate of 20 °C min^{-1}, and kept at 1000 °C for 10 min to anneal the templates. After annealing, the carbon precursor CH_4 was introduced at a flow rate of 21 ml min^{-1}, equivalent to 3 vol % of CH_4 in the mixed gas. The grow of graphene layers on the surface of compressed Ni foams lasted for 15 min at 1000 °C followed by rapid cooling of the tube to room temperature under the mixed gas flow of Ar (500 ml min^{-1}) and H_2 (200 ml min^{-1}). The graphene-Ni foams were removed from the tube and immersed into a mixed solution of 3 M HCl and 0.5 M $FeCl_3$ to etch out the Ni templates at 80 °C on a hot plate. Freestanding MGWs were collected from the solution and rinsed in DI water three times before drying in an oven at 60 °C overnight.

The epoxy resin (LY1564, Huntsman Advanced Materials) and the hardener (XB 3403, Huntsman Advanced Materials) were mixed at a weight ratio of 100:12 in a beaker and mechanically stirred at 40 °C for 30 min on a hot plate. The freestanding MGWs were placed in a mold and the mixture of resin and hardener was poured into the mold to impregnate the MGWs. The prepreg was then degassed in a vacuum oven at 40 °C for 3 h to ensure that the open cellular and hollow graphene struts in MGWs were fully infiltrated by the epoxy. After degassing, the prepreg was transferred to a stainless-steel mold and cured at 80 °C for 0.5 h and post-cured at 120 °C for 1.5 h. For comparison, cellular GFs were also prepared using the original, uncompressed Ni foams to fabricate GF/epoxy composites following the same procedure. Composite samples with varying graphene contents were prepared using MGWs with different densities.

Characterizations. The morphologies of GFs and MGWs and their epoxy composites were characterized using SEM (JEOL-6390) and TEM (JEOL 2010F). The thickness of graphene

strut walls was characterized using a Raman spectrometer (Renishaw micro-Raman). The electrical conductivities of MGWs and their composites were measured at room temperature using a four-probe resistivity measurement system. The samples were cut into squares of 10 mm × 10 mm, and the contact surfaces were coated with silver paste to reduce the resistance between the probe and surface. The thermal conductivities of composites were measured using the laser flash method.[1] The thermal conductivity, κ, is expressed as

$$\kappa = C_p \rho \alpha, \quad \text{(S1)}$$

where C_p is the specific heat capacity, ρ is the density and α is the thermal diffusivity. The thermal diffusivities of composite samples both in the plane and thickness directions were measured using a laser flash apparatus (LFA-447, NETZSCH) according to ASTM E1461. Disk-shape samples with a diameter of 25.4 mm and a thickness of 0.4 mm were used for in-plane thermal diffusivity measurements while those with a diameter of 12.8 mm and a thickness of 1 mm for through-the-thickness measurements. The heat capacity was measured using a differential scanning calorimeter (DSC, TA-Q1000) and the density was calculated from the mass and the volume of the samples.

S2. Analytical model for thermal conductivities of anisotropic MGW/epoxy composites

The thermal conductivities of composites containing isotropic continuous GF with a volume fraction of f can be obtained by:[2]

$$\kappa_c = \kappa_{foam} + (1 - f)\, \kappa_{ep}, \quad \text{(S2)}$$

where f is the volume fraction of graphene, κ_{ep} is the thermal conductivity of the epoxy matrix, and $\kappa_{foam}$is the thermal conductivity of isotropic GF. κ_{foam} was related to the thermal conductivity of graphene strut, κ_G, according to the metal foam theory:[1]

$$\kappa_{foam} = \frac{1}{3} f \kappa_G, \quad \text{(S3)}$$

where the coefficient of 1/3 reflects the random orientation of the graphene struts. To obtain the value of κ_G, the thermal conductivity of GF/epoxy composites with a graphene content of 0.65 wt % was measured using the laser flash technique, which was 0.72 ± 0.26 $Wm^{-1}K^{-1}$. The thermal conductivity of epoxy matrix measured from the laser flash technique was κ_{ep}=0.18 ± 0.05 $Wm^{-1}K^{-1}$. Therefore, the thermal conductivity of solid graphene strut obtained from equation (S2) and (S3) was κ_G = 460 $Wm^{-1}K^{-1}$. This value was used for all the subsequent calculations of the thermal conductivities of anisotropic MGW/epoxy composites.

To calculate the thermal conductivities of anisotropic MGW/epoxy composites, two orientation parameters, μ_i and ξ, were introduced. The exact values of $\mu_i$corresponding to each orientation state shown in Figure 4b were obtained from the in-plane orientation parameter,[2] $f_p = 2\langle \cos^2 \theta_i \rangle - 1$, and the out-of-plane orientation parameter,[2] $f_a = \frac{3\langle \cos^2 \theta_i \rangle - 1}{2}$. In the case of in-plane 2D random orientation (*i.e.*, Case II in Figure 4b), $f_p = 0$ indicates a random distribution of graphene struts in the horizontal plane. Thus, for graphene struts in Group 1, $\mu_1 = \langle \cos^2 \theta_1 \rangle = \frac{(f_p + 1)}{2} = \frac{1}{2}$. For graphene struts in Group 2, random orientations give $\mu_2 = \langle \cos^2 \theta_2 \rangle = \frac{1}{3}$. Hence, the in-plane thermal conductivity, $\kappa_{in-plane}$, is

$$\kappa_{in-plane} = \frac{1}{2}\xi f \kappa_G + \frac{1}{3}(1-\xi) f \kappa_G + (1-f)\,\kappa_{ep}, \quad \text{(S4)}$$

Similarly, the value of μ_1 for calculating the transverse thermal conductivities, κ_{trans}, was obtained from the out-of-plane orientation parameter, f_a. A value of $f_a = -0.5$ indicates all the elements were perpendicular to the vertical axis and contained within the horizontal plane,[3] corresponding to the case of graphene struts in Group 1. This gives $\mu_1 = \langle \cos^2 \theta_1 \rangle = 0$. For graphene struts in Group 2, random orientations give $\mu_2 = \langle \cos^2 \theta_2 \rangle = \frac{1}{3}$. Hence,

$$\kappa_{trans} = \frac{1}{3}(1-\xi)f\kappa_G + (1-f)\,\kappa_{ep}. \quad \text{(S5)}$$

For the perfectly aligned case (*i.e.*, Case I in Figure 4b), in-plane orientation parameter f_p equals 1. This leads to orientation parameters $\mu_1 = \mu_2 = 1$ for both Group 1 and 2. Hence, the thermal conductivity of composite with aligned graphene struts is:

$$\kappa_{aligned} = \frac{1}{2}\xi f\kappa_G + \frac{1}{3}(1-\xi)f\kappa_G + (1-f)\,\kappa_{ep}. \quad \text{(S6)}$$

When graphene struts in both Group 1 and 2 are completely randomly oriented (*i.e.*, Case III in Figure 4b), the values of both orientation parameters, μ_1 and μ_2, are 1/3. Therefore, the thermal conductivity of composite containing randomly oriented graphene struts can be calculated by

$$\kappa_{random} = \frac{1}{3}\xi f\kappa_G + \frac{1}{3}(1-\xi)f\kappa_G + (1-f)\,\kappa_{ep} = \frac{1}{3}f\kappa_G + (1-f)\,\kappa_{ep}, \quad \text{(S7)}$$

which reduces to Equation (S2).

S3. Measurement of fracture toughness

The single-edge-notch bending (SENB) tests were carried out to measure the quasi-static fracture toughness, K_{Ic}, of MGW/epoxy composites according to ASTM standard D5045. The dimension of the specimen is 47 mm long × 10.8 mm wide × 5.4 mm thick and a pre-crack of 5.4 mm deep was made by first using a razor notching machine (CEAST) and then tapping a fresh razor blade into the existing notch (Figure S4). A universal testing machine (MTS Alliance RT/10) was used to test the specimen in three-point bending at a crosshead speed of 10 mm min^{-1}. The load-displacement curve was obtained and the fracture toughness, K_{Ic}, was determined by:

$$K_{Ic} = \left(\frac{P_Q}{BW^{\frac{1}{2}}} \right) f(a/W) \quad . \tag{S8}$$

In the above equation, W and B are the width and thickness of the specimen, respectively; a is the crack length; P_Q is the force determined from the load-displacement curve; and $f(a/W)$ is defined as

$$f\left(\frac{a}{W}\right) = 6\left(\frac{a}{W}\right)^{1/2} \frac{\left[1.99 - \frac{a}{W}(1 - \frac{a}{W})(2.15 - 3.93\frac{a}{W} + 2.7\left(\frac{a}{W}\right)^2)\right]}{(1 + 2\frac{a}{W})(1 - \frac{a}{W})^{3/2}} \quad . \tag{S9}$$

The validity of each test was checked by comparing P_Q and the maximum load, P_{max}, in the load displacement curve, according to the specification. At least four specimens were tested for each set of conditions for a given graphene content.

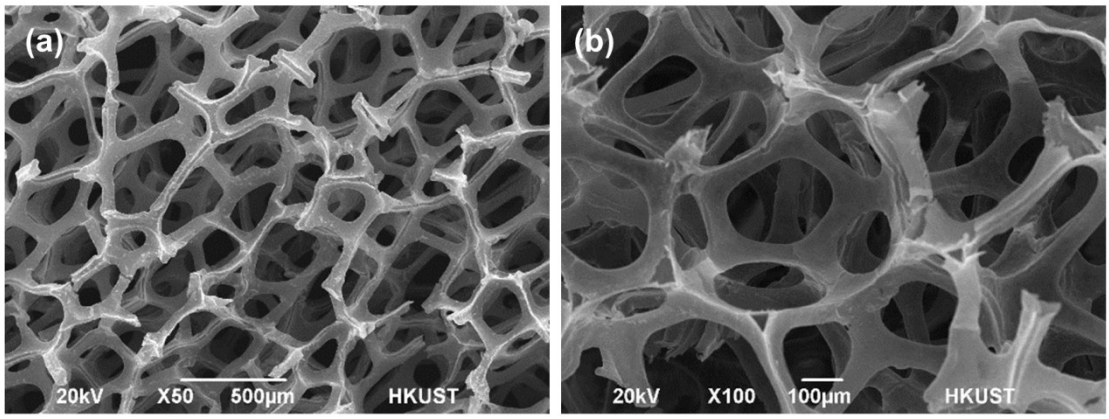

Figure S1. SEM images of the (a) surface and (b) cross-section of GF showing the isotropic morphology on a macroscopic scale.

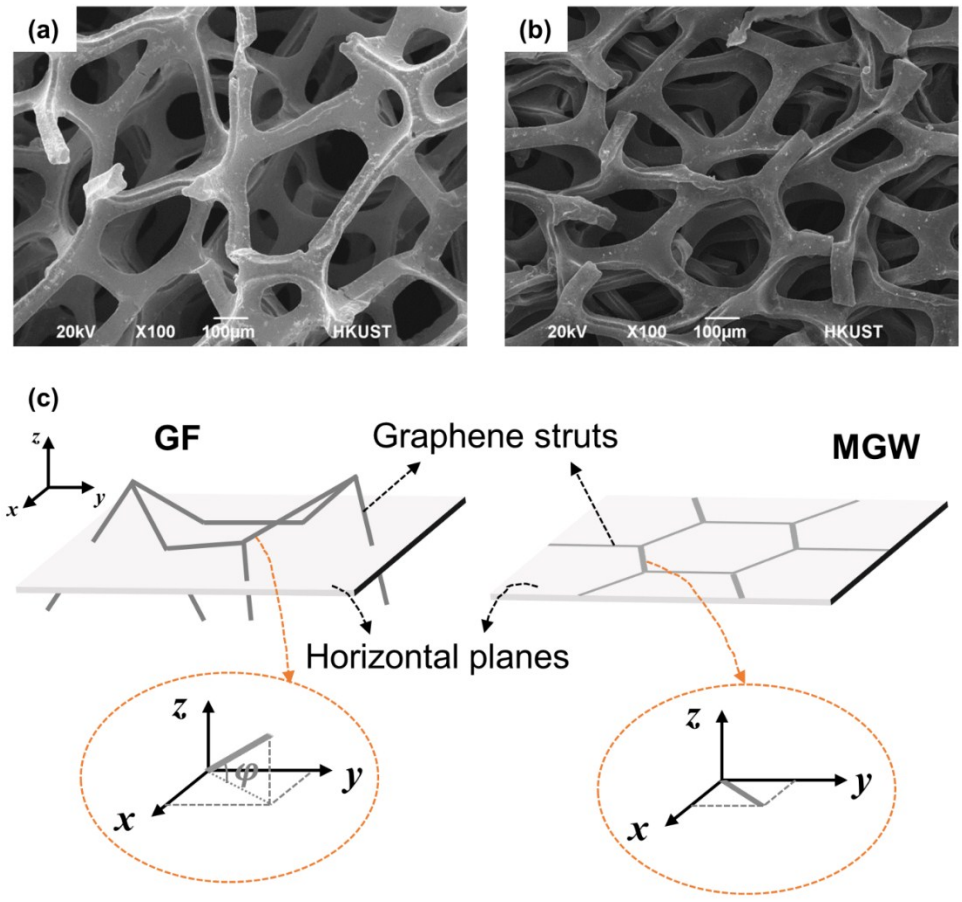

Figure S2. SEM images of top surfaces of (a) pristine GF and (b) MGW. The graphene struts in GF are randomly oriented in 3D space whereas the majority of those in MGW are oriented in the horizontal plane. (c) Schematics showing the orientation of graphene struts in GF and

MGW. The graphene struts in GF show an angle, φ, with respect to the horizontal plane (*i.e.*, *x*-*y* plane), while the angle between a graphene strut in MGW and the horizontal plane is nearly zero.

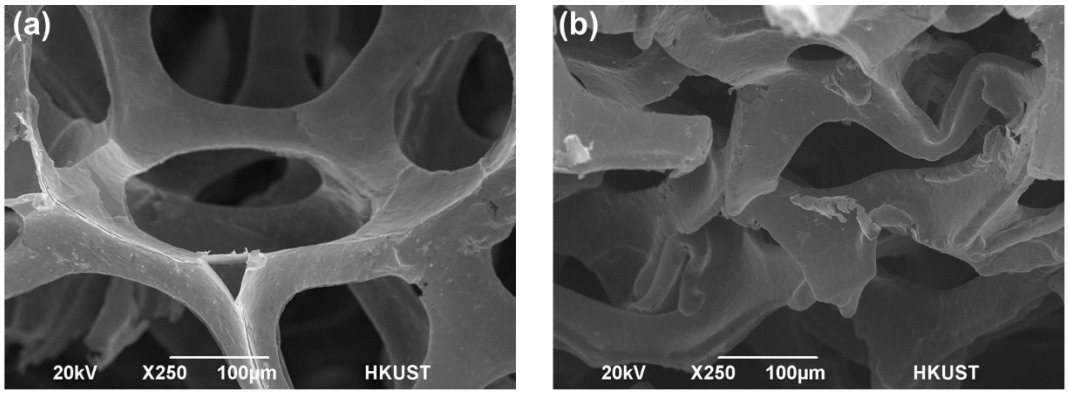

Figure S3. Cross-sectional SEM images showing the shape of graphene struts in (a) pristine GF and (b) MGW with a density of 62.3 mg cm^{-3}.

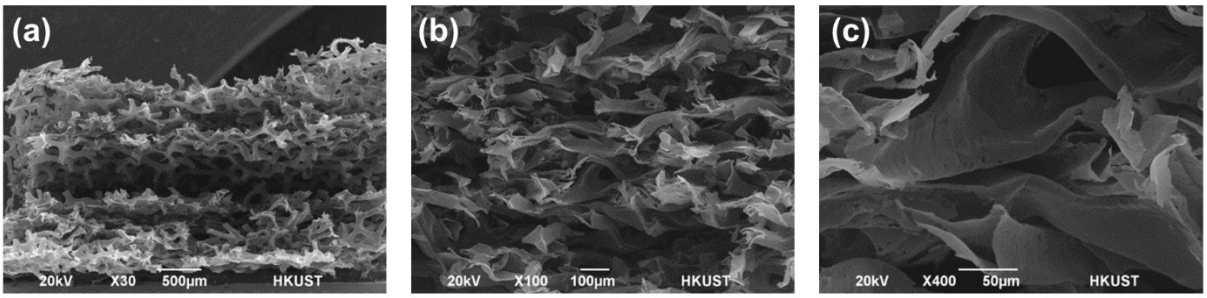

Figure S4. (a) SEM images of the torn cross-section of MGW made from 4 layers of compressed Ni foams. Delamination occurs at the edge upon tearing, indicating lack of intermingling between layers. (b-c) High-magnification SEM images of the torn cross-section of MGW made from 8 layers of compressed Ni foams. The individual layers are intermingled one other without clear interfaces, signifying seamless interconnection through the whole thickness.

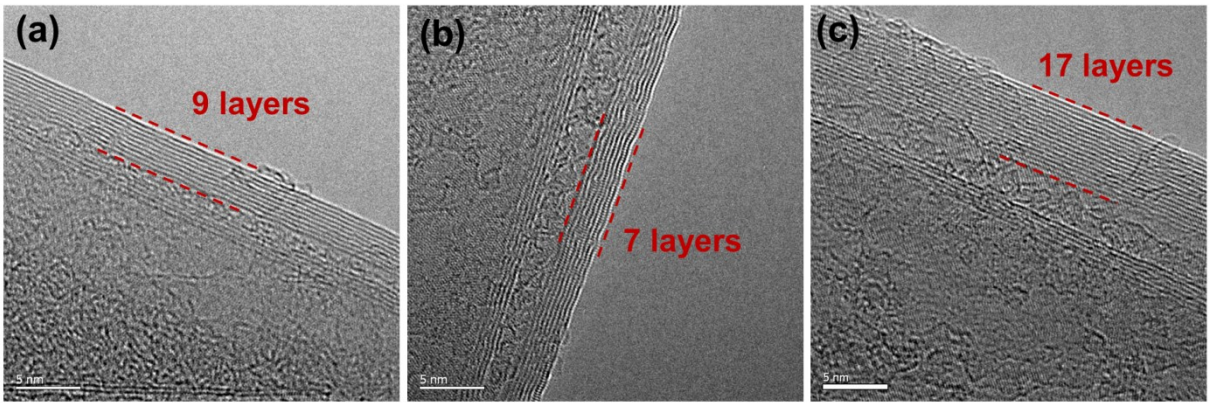

Figure S5. Typical TEM images of graphene strut walls with (a) 9, (b) 7 and (c) 17 graphene layers.

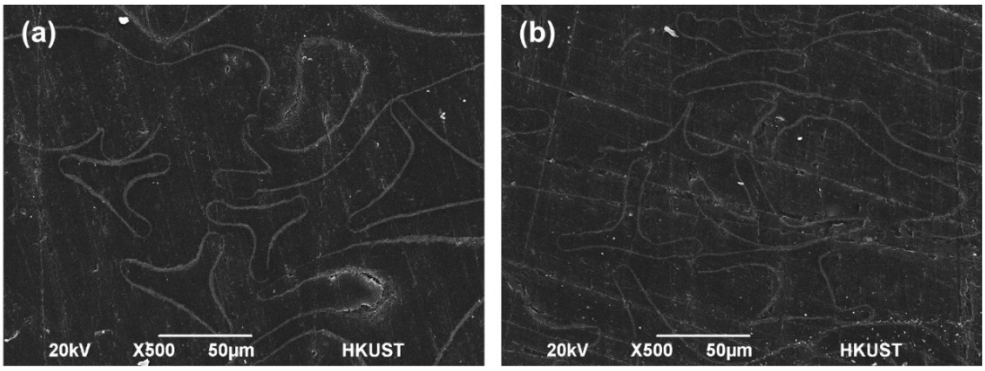

Figure S6. SEM images of polished surfaces of MGWs/epoxy composites with graphene contents of (a) 2.8 wt % and (b) 5.5 wt %.

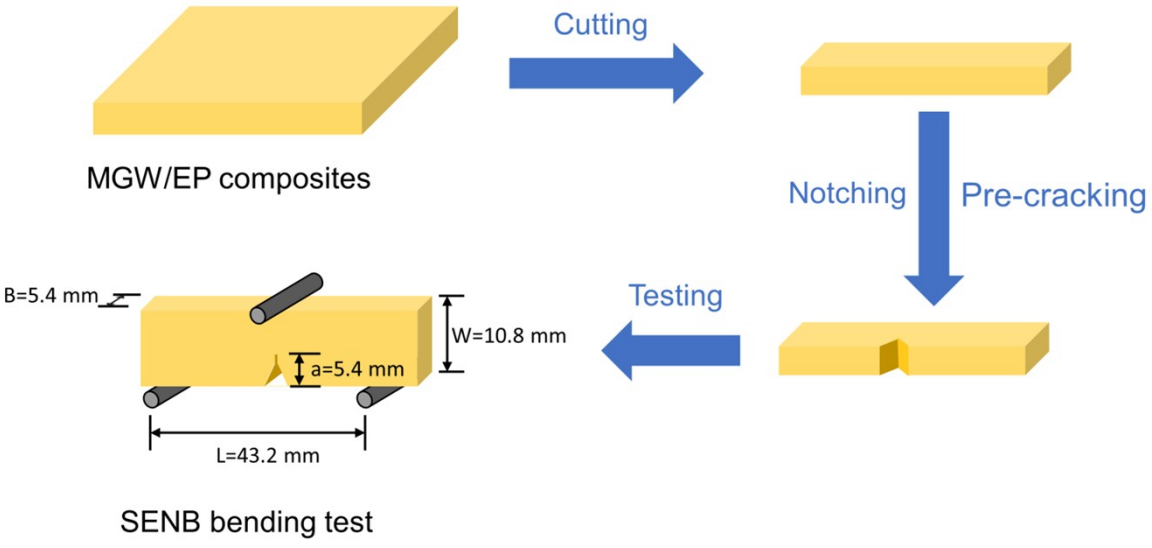

Figure S7. Schematics of the preparation of samples for SENB tests.

Table S1. Comparison of electrical conductivities of epoxy composites containing different carbon nano-fillers.

Type of fillers	Filler content (wt %)	Electrical conductivity (S cm^{-1})	Ref
GF	0.65	4.5	This work
MGW	2.23	15.9	This work
	2.82	24.7	
	5.48	38.9	
	8.32	50.3	
GF	0.11	1	[23]
	0.16	1.2	
	0.2	3	
	0.38	3.5	
	0.45	3.5	
	0.53	3.6	
GWF	0.19	0.15	[28]
	0.24	0.16	
	0.31	0.16	
	0.4	0.17	
	0.52	0.17	
	0.62	0.18	
GA	0.25	0.0018	[13]
	0.35	0.0056	
	0.49	0.0091	

	0.64	0.0150	
	0.8	0.0298	
	1.02	0.0732	
	1.36	0.2010	
GNP	0.1	3×10^{-11}	[42]
	0.3	2×10^{-7}	
	0.5	1×10^{-5}	
	1	1.8×10^{-5}	
	2	5.8×10^{-5}	
rGO	0.2	1×10^{-11}	[6]
	0.25	9×10^{-8}	
	0.3	2×10^{-6}	
	0.4	5×10^{-6}	
	0.5	1×10^{-5}	
	0.75	1×10^{-4}	
	1	2×10^{-4}	
	1.5	8×10^{-4}	
	2	8×10^{-3}	
	3	0.008	
SWCNT	0.2	2×10^{-10}	[39]
	0.5	5×10^{-9}	
	1	6×10^{-8}	
	3	1×10^{-6}	
CNT	0.05	8×10^{-13}	[40]
	0.1	1×10^{-8}	

	0.25	2×10^{-4}	
	0.5	7×10^{-4}	
	1	0.004	
CNF	0.3	3.5×10^{-12}	[41]
	0.6	2.1×10^{-10}	
	1.2	5.3×10^{-8}	
	2	1.0×10^{-6}	

Table S2. Comparison of thermal conductivities of MGW/epoxy composites with others containing different types of graphene.

Type of composites	Filler content (wt %)	Thermal conductivity (Wm^{-1} K^{-1})	Ref
MGW/EP	2.23	5.058	This work
	2.82	5.862	
	5.48	7.263	
	8.32	8.849	
GF/wax	0.83	1.65	[24]
	1.23	3.61	
GF-MLG/EP	2	0.55	[26]
Random GA/EP	0.36	0.20	[15]
	0.84	0.22	
	0.95	0.23	
	1.26	0.27	
	1.37	0.36	

	1.67	0.45	
Aligned GA/EP	0.36	0.22	[15]
	0.84	0.45	
	0.95	0.72	
	1.26	0.77	
	1.37	1.10	
	1.67	2.13	
MLG/EP	2.73	0.65	[44]
	3.61	0.8	
	5.4	1.23	
	7.1	1.8	
	8.8	2.65	
	10.48	2.9	
f-G/EP	10	1.53	[45]
High-aspect-ratio			[34]
GNP/EP	1	0.339	
	2	0.696	
	5	1.473	
GNP/EP	13.75	2	[7]
	20	2.4	
	24.4	3.4	
	28.7	4.1	
	31.43	6.6	
	36.7	12.4	

Table S3. Comparison of enhancement in K_{Ic} of different epoxy composites.

Type of composites	Filler content (wt %)	K_{Ic} (MPa $m^{1/2}$)	Enhancement in K_{Ic} (%)	Ref.
GF/EP	0.62	1.56	48.6	This work
MGW/EP	2.2	2.03	93.3	This work
	2.8	2.04	94.3	
	5.4	2.12	102.0	
	8.3	2.18	107.6	
GF/EP (porous)	0.1	1.78	70	[23]
	0.16	1.76	67.5	
	0.2	1.76	67.5	
	0.38	1.79	69	
	0.45	1.75	65	
	0.53	1.71	60	
GWF/EP (porous)	0.31	1.54	44.5	[28]
	0.4	1.6	49.7	
	0.52	1.66	56	
	0.62	1.78	66.5	
GA/EP	0.3	1.45	48	[13]
	0.5	1.5	52	
	0.8	1.55	60	
	1.3	1.58	63	

GNP/EP	0.1	0.76	52	[51]
	0.5	0.80	60	
	1	0.84	68	
	2	0.91	82	
f-GNP/EP	1	0.76	10	[52]
	2.6	1.01	46.4	
	4	1.32	91.3	
	5.5	1.27	84.1	
GO/EP	0.1	0.95	28	[50]
	0.25	1.1	49	
	0.5	1.21	63	
	1	1.18	60	
CNT/EP	0.1	0.85	23.2	[49]
	0.2	0.88	27.5	
	0.5	0.98	42	

References

(1) X. Shen, Z. Wang, Y. Wu, X. Liu, Y.-B. He and J.-K. Kim, *Nano Lett.*, 2016, **16**, 3585–3593.

(2) Ji, H.; Sellan, D. P.; Pettes, M. T.; Kong, X.; Ji, J.; Shi, L.; Ruoff, R. S. *Energy Environ. Sci.* **2014**, *7* (3), 1185.

(3) Li, J.; Kim, J.-K. *Compos. Sci. Technol.* **2007**, *67* (10), 2114–2120.